Available online at www.sciencedirect.com

ScienceDirect

International Journal of Thermal Sciences 47 (2008) 560–568

International Journal of Thermal Sciences

www.elsevier.com/locate/ijts

Investigations of thermal conductivity and viscosity of nanofluids

S.M.S. Murshed, K.C. Leong *, C. Yang

School of Mechanical and Aerospace Engineering, Nanyang Technological University, 50 Nanyang Avenue, Singapore 639798, Republic of Singapore

Received 17 September 2006; received in revised form 5 May 2007; accepted 7 May 2007

Available online 29 June 2007

Abstract

A combined experimental and theoretical study on the effective thermal conductivity and viscosity of nanofluids is conducted. The thermal conductivity and viscosity of nanofluids are measured and found to be substantially higher than the values of the base fluids. Both the thermal conductivity and viscosity of nanofluids increase with the nanoparticle volume fraction. The thermal conductivity of nanofluids was also observed to be strongly dependent on temperature. Two static mechanisms-based models are presented to predict the enhanced thermal conductivity of nanofluids having spherical and cylindrical nanoparticles. The proposed models show reasonably good agreement with the experimental results and give better predictions for the effective thermal conductivity of nanofluids compared to existing classical models. Based on the calibration results from the transient hot-wire method, the measurement error was estimated to be within 2%. In addition, the measured values of the effective viscosity of nanofluids are found to be underestimated by classical models.

Keywords: Nanofluids; Thermal conductivity; Viscosity

1. Introduction

Nanofluids, which are suspensions of nanoparticles in conventional fluids such as water, ethylene glycol and engine oil, have attracted great interest from many researchers due to their potential benefits and applications in important fields such as microelectronics, energy supply, transportation and HVAC. From investigations in the past decade [1–6], nanofluids were found to exhibit substantially higher thermal properties particularly thermal conductivity even when the concentrations of suspended nanoparticles are very low ($\phi < 5\%$). However, the increments of thermal conductivities are different for different types of nanofluids. The thermal conductivity of nanofluids varies with the size, shape, and material of nanoparticles. For example, nanofluids with metallic nanoparticles were found to have a higher thermal conductivity than nanofluids with nonmetallic (oxide) nanoparticles. The smaller the particle size, the higher the thermal conductivities of nanofluids. Furthermore, nanofluids with spherical shape nanoparticles exhibit a smaller increase in thermal conductivity compared with the nanofluids having cylindrical (nano-rod or tube) nanoparticles [7]. In addition, temperature may play an important role in enhancing the effective thermal conductivity of nanofluids. As reported in the literature, most experimental studies on the determination of the thermal conductivity of nanofluids have been conducted at room temperature. Very few studies [5,8,9] have been performed to investigate the temperature effect on the effective thermal conductivity of nanofluids. Hence, to confirm the effects of these parameters on the effective thermal conductivity of nanofluids, more experimental studies are essential. Thus, in this paper, the effective thermal conductivity of several types of nanofluids was measured by the transient hot-wire method at different temperatures. The existing classical models such as those attributed to Maxwell [10], Hamilton–Crosser (HC) [11] and Bruggeman [12] were found to be unable to predict the anomalously high thermal conductivity of nanofluids. This is because these classical models do not include the effects of particle size, distribution and the interfacial layer at the particle/liquid interface which are considered as important mechanisms for enhancing thermal conductivity of nanofluids [13–18]. The thermophysical properties of the interfacial layer are different from the bulk liquid and solid particles. Specifically, in the present study the interfa-

---

* Corresponding author. Tel.: +65 6790 4725; fax: +65 6792 2619.
E-mail address: mkcleong@ntu.edu.sg (K.C. Leong).

1290-0729/$ – see front matter © 2007 Elsevier Masson SAS. All rights reserved.
doi:10.1016/j.ijthermalsci.2007.05.004

Nomenclature

a	Particle radius	m
E_∞	External temperature field	$\mathrm{K\,m^{-1}}$
h	Interfacial layer thickness	m
k	Thermal conductivity	$\mathrm{W\,m^{-1}\,K^{-1}}$
T	Temperature	K
η	Viscosity	Pa s
ϕ	Volume fraction	

Subscripts

eff	Effective
f	Base fluid
lr	Interfacial layer
m	Maximum
p	Particle

cial layer is considered as a separate component in the model development in order to determine the effective thermal conductivity of nanofluids. The results predicted by the present models were analyzed and compared with the experimental results.

While the prediction and measurement of the effective thermal conductivity of nanofluids have received much attention in recent years, very few studies [2,19] have been performed on effective viscosity, which influences the flow and heat transfer characteristics. Thus, in this study, the effective viscosity of nanofluids are measured and compared with values predicted by classical models as well as experimental data obtained from the literature.

2. Theoretical

2.1. Modeling the effective thermal conductivity

A sketch of a nanoparticle with an interfacial layer in a fluid medium is shown in Fig. 1. The components (three regions) and their parameters are: (1) the particle (p) with radius a, thermal conductivity k_p and temperature T_p, (2) the interfacial layer (lr) between particle/fluid medium with thickness h, thermal conductivity k_lr and temperature T_lr, and (3) the fluid medium (f) with thermal conductivity k_f and temperature T_f.

The following assumptions are made for the model development:

1. The mixture (nanofluids) includes three components, namely particle, interfacial layer, and liquid.
2. The stationary nanoparticles are apart from each other.
3. The temperature fields are continuous in all three components and at the interfacial boundaries and the heat fluxes across the interfaces (particle/layer and layer/fluid) are also continuous.

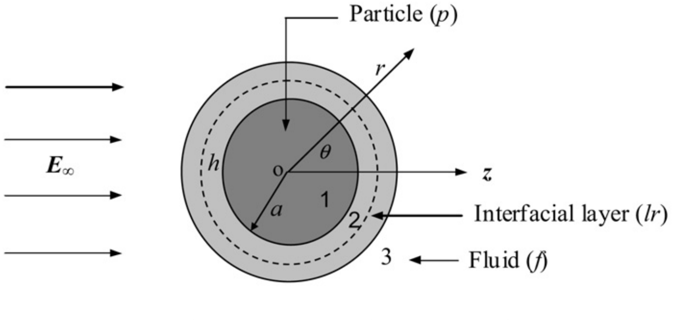

Fig. 1. Sketch of a particle with interfacial layer in a fluid medium.

The two-dimensional (r and θ), steady-state heat conduction equation (i.e. the Laplace equation) is given by

$$\nabla^2 T = 0 \tag{1}$$

By considering the uniform external temperature field E_∞ along any direction (e.g. along the z axis in this case), the boundary conditions are as follows:

$$T_\mathrm{p}|_{r\to 0} = \text{const.} \quad \text{at the particle center} \tag{2}$$

$$T_\mathrm{f}|_{r\to\infty} = E_\infty z \quad \text{at a large distance} \tag{3}$$

$$T_\mathrm{p}|_{r=a} = T_\mathrm{lr}|_{r=a} \quad \text{at the particle/layer interface} \tag{4a}$$

$$-k_\mathrm{p}\frac{\mathrm{d}T_\mathrm{p}}{\mathrm{d}r}\bigg|_{r=a} = -k_\mathrm{lr}\frac{\mathrm{d}T_\mathrm{lr}}{\mathrm{d}r}\bigg|_{r=a} \quad \text{at the particle/layer interface} \tag{4b}$$

$$T_\mathrm{lr}|_{r=a+h} = T_\mathrm{f}|_{r=a+h} \quad \text{at the layer/liquid interface} \tag{5a}$$

$$-k_\mathrm{lr}\frac{\mathrm{d}T_\mathrm{lr}}{\mathrm{d}r}\bigg|_{r=a+h} = -k_\mathrm{f}\frac{\mathrm{d}T_\mathrm{f}}{\mathrm{d}r}\bigg|_{r=a+h} \quad \text{at the layer/liquid interface} \tag{5b}$$

With the boundary conditions, Eq. (1) was solved for both the spherical and the cylindrical coordinates systems and the temperature gradients in each component were then obtained. By making use of the temperature gradients and spatial averages of the heat fluxes in all components, two models for the effective thermal conductivities of nanofluids with spherical and cylindrical nanoparticles were obtained as follows:

$$\begin{aligned} k_\mathrm{eff} = \big(&(k_\mathrm{p} - k_\mathrm{lr})\phi_\mathrm{p} k_\mathrm{lr}\big[2\gamma_1^3 - \gamma^3 + 1\big] + (k_\mathrm{p} + 2k_\mathrm{lr}) \\ &\times \gamma_1^3\big[\phi_\mathrm{p}\gamma^3(k_\mathrm{lr} - k_\mathrm{f}) + k_\mathrm{f}\big]\big)\big(\gamma_1^3(k_\mathrm{p} + 2k_\mathrm{lr}) \\ &- (k_\mathrm{p} - k_\mathrm{lr})\phi_\mathrm{p}\big[\gamma_1^3 + \gamma^3 - 1\big]\big)^{-1} \end{aligned} \tag{6}$$

for spherical coordinates,

$$\begin{aligned} k_\mathrm{eff} = \big(&(k_\mathrm{p} - k_\mathrm{lr})\phi_\mathrm{p} k_\mathrm{lr}\big[\gamma_1^2 - \gamma^2 + 1\big] + (k_\mathrm{p} + k_\mathrm{lr}) \\ &\times \gamma_1^2\big[\phi_\mathrm{p}\gamma^2(k_\mathrm{lr} - k_\mathrm{f}) + k_\mathrm{f}\big]\big)\big(\gamma_1^2(k_\mathrm{p} + k_\mathrm{lr}) \\ &- (k_\mathrm{p} - k_\mathrm{lr})\phi_\mathrm{p}\big[\gamma_1^2 + \gamma^2 - 1\big]\big)^{-1} \end{aligned} \tag{7}$$

for cylindrical coordinates where $1 + \frac{h}{a} = \gamma$ and $1 + \frac{h}{2a} = \gamma_1$.

The detailed discussion and mathematical derivations for the spherical nanoparticles are provided by Leong et al. [20]. It is noticed that these models given by Eqs. (6) and (7) are based on static mechanisms of nanoparticles in base fluids.

There is no exact theoretical model available to determine the thickness of the nanolayer at the nanoparticle–liquid interface. Based on the electron density profile at the interface, Hashimoto et al. [21] established a model for the interfacial layer thickness at the surface of microdomains, which is given as

$$h = \sqrt{2\pi}\sigma \tag{8}$$

where σ is a parameter which characterizes the diffuseness of interfacial boundary and its typical value is within 0.2–0.8 nm. By extending the Debye equation, Li et al. [22] also introduced the same model for the determination of interfacial layer thickness of a solid–liquid system. For $\sigma = 0.4$ nm, Eq. (8) yields the interfacial layer thickness to be 1 nm. In fact, the experimental results of Yu et al. [23] and the molecular dynamic simulations performed by Xue et al. [24] showed that the typical solid-like interfacial layer width is of the order of a few atomic distances i.e. ≈1 nm. Moreover, the effect of interfacial layer thickness within 1–2 nanometers is not significant in the present models. Therefore, as calculated from Eq. (8), the interfacial layer thickness of 1 nm for spherical particle and 2 nm for carbon nanotubes will be used to predict the thermal conductivity of nanofluids by the present models.

2.2. *Models for the effective viscosity*

On top of very few experimental studies, no established model is available for the prediction of the effective viscosity of nanofluids. The Einstein model [18] is commonly used to predict the effective viscosity of suspensions containing a low volume fraction of particles (usually <0.01). Since the particle volume fractions used in this study are between 0.01 and 0.05, the power law based models [25,26] are more appropriate for the prediction of the effective viscosity of nanofluids compared to the Einstein model. For simple hard sphere systems, the relative viscosity (the ratio of the effective viscosity of suspension, η_{eff} to that of the suspending medium, η_{f}) increases with particle volume fraction, ϕ_{p}. To determine this relative viscosity, a semi-empirical equation formulated by Krieger and Dougherty (K–D) [25] expressed as

$$\frac{\eta_{\mathrm{eff}}}{\eta_{\mathrm{f}}} = \left(1 - \frac{\phi_{\mathrm{p}}}{\phi_{\mathrm{m}}}\right)^{-[\eta]\phi_{\mathrm{m}}} \tag{9}$$

is used where ϕ_{m} is the maximum packing fraction and $[\eta]$ is the intrinsic viscosity ($[\eta] = 2.5$ for hard spheres). For randomly mono-dispersed spheres, the maximum close packing fraction is approximately 0.64 [25].

A decade later, a generalized equation for the relative elastic moduli of composite materials (also widely used for relative viscosity) was proposed by Nielsen [26]. For a concentration of dispersed particles, Nielsen's equation can be simplified as follows:

$$\frac{\eta_{\mathrm{eff}}}{\eta_{\mathrm{f}}} = (1 + 1.5\phi_{\mathrm{p}})\mathrm{e}^{\phi_{\mathrm{p}}/(1-\phi_{\mathrm{m}})} \tag{10}$$

where ϕ_{p} and ϕ_{m} are the volume fraction of particles and the maximum packing fraction, respectively. In this study, these two models [Eqs. (9) and (10)] are used to predict the effective viscosity of nanofluids. It is noted that the Einstein model yields slightly lower values of effective thermal conductivity than the K–D model.

3. Experimental

The transient hot-wire technique was used to measure the thermal conductivity of nanofluids at different temperatures ranging from 20–60 °C. The transient hot-wire technique is more appropriate than the steady-state technique due to numerous advantages such as the elimination of natural convection effects and faster experimental response. Fig. 2 shows the experimental setup. The measurement procedure and details of the transient hot-wire technique can be found in our previous work [7] where the experiments were conducted at room temperature. In addition to the hot-wire system, a refrigerating/heating circulator was used to maintain different temperatures in the nanofluids during the present experiments (Fig. 2). The experimental apparatus was calibrated by measuring the effective thermal conductivity of the base fluids, i.e. deionized water, ethylene glycol and engine oil in this case. Based on the calibration results from the transient hot-wire method for the base

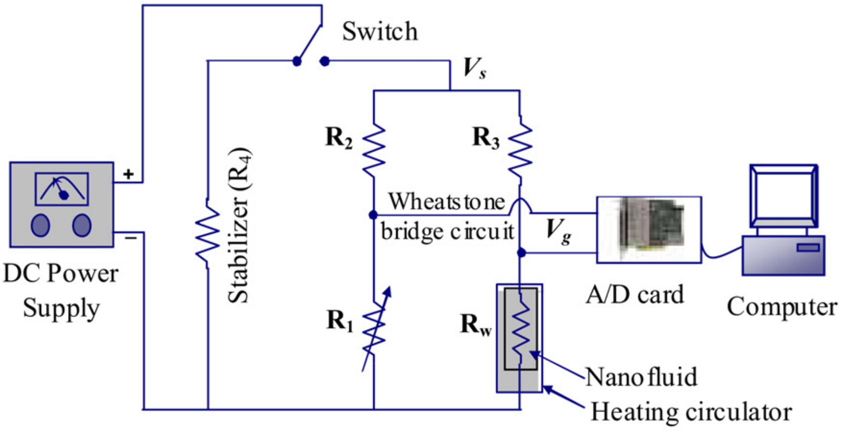

Fig. 2. Schematic of the transient hot-wire experimental setup.

fluids, the measurement error was estimated to be within 2%. All measurements were performed at atmospheric pressure.

Sample nanofluids were prepared by suspending different volume percentages (1 to 5%) of oxide nanoparticles such as titanium dioxide and aluminum oxide nanoparticles in deionized water (DIW) and ethylene glycol. Nanofluids with metallic nanoparticles were also prepared by dispersing aluminum (Φ80 nm) nanoparticles in ethylene glycol (EG) and engine oil (EO). To ensure proper dispersion of nanoparticles, the sample nanofluids were homogenized by using an ultrasonic dismembrator before the experiments were conducted. Cetyl Trimethyl Ammonium Bromide (CTAB) surfactant (about 0.1 mM) was added to ensure better stability and dispersion of nanoparticles in the base fluids. The surfactant keeps particles dispersed in base fluids by electrostatic repulsive forces among the particles and hydrophobic surface forces due to physical adsorption of surfactant in the solution.

The effective viscosity of several nanofluids was also measured by a controlled rate rheometer and the results were compared with those predicted by the existing models.

4. Results and discussion

The measured and predicted effective thermal conductivity and viscosity of several nanofluids are presented. The results predicted by the present and existing models are compared with our experimental results as well as data from the literature. The experimental results show a substantial increase in thermal conductivity with the particle volume fraction. From Fig. 3, it can be seen that the maximum increase of thermal conductivity of TiO_2 (15 nm)/ethylene glycol-based nanofluids is 18% for the particle volumetric loading of 5% while Fig. 4 shows 45% increase for the same volume fraction of Al (80 nm) nanoparticles in ethylene glycol. As shown in Figs. 3 and 4, nanofluids having higher thermally conductive nanoparticles (Al) exhibit much higher thermal conductivity compared to the nanofluids having lower thermally conductive nanoparticles (TiO_2). It can also be seen that the present model for spherical nanoparticle shows reasonably good agreement with the experimental results and gives better predictions for the effective thermal conductivity of nanofluids compared to Maxwell [10] and Prasher et al.'s [27] models. For spherical particles, the Hamilton–Crosser (HC) model is the same as the Maxwell model. Although Prasher et al.'s (2005) model considered the effect of particle size and microconvection, it cannot predict the thermal conductivity of these nanofluids (Figs. 3 and 4). This is because it did not consider the effect of interfacial layer and the suggested values of fitting parameters may not be valid for these nanofluids. It is noted that suggested values of three unknown parameters (i.e. interfacial resistance, $R_b = 1.2 \times 10^{-8}\ \mathrm{K\,m^2\,W^{-1}}$, constants $A = 40\,000$ and $m = 1.6$) are used for the calculation of the thermal conductivity of ethylene glycol-based nanofluids. Currently, the values of these unknown parameters cannot be obtained by experimental or theoretical means.

The predictions by the present model for cylindrical nanoparticles were also compared with the experimental data of Choi et al. [3] for carbon nanotubes (25 nm × 50 µm)/engine oil (EO)-based nanofluids as shown in Fig. 5. The agreement is satisfactory because the present model shows closer agreement with the experimental data. It can also be seen from Fig. 5 that the Hamilton–Crosser (HC) model severely under-predicts the effective thermal conductivity of this nanofluid. This is probably due to the limitation of the Hamilton–Crosser model which reaches its maximum enhancement in thermal conductivity

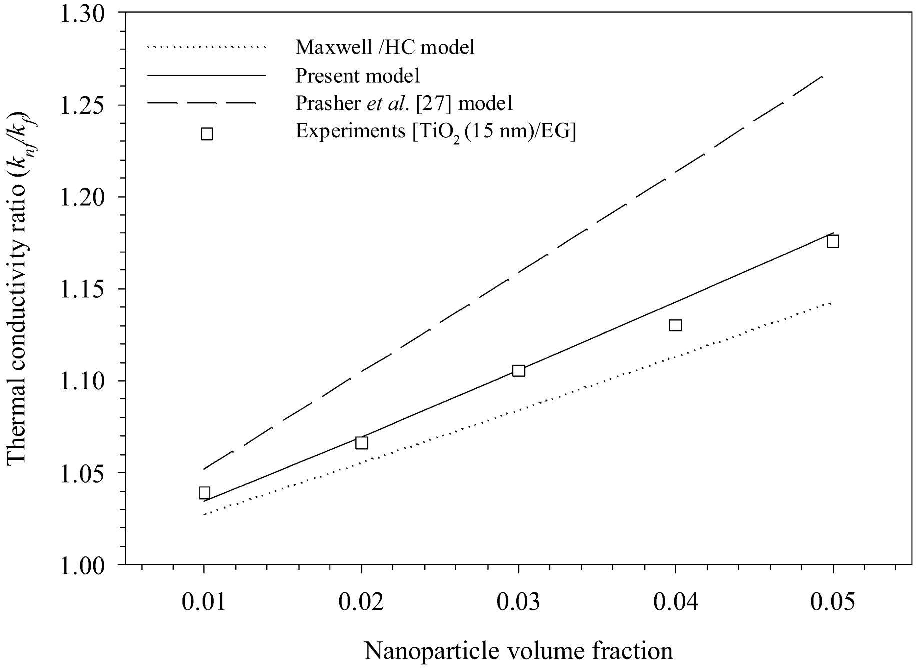

Fig. 3. Comparison of present model [Eq. (6)] predictions ($k_{\mathrm{lr}} = 1.25k_{\mathrm{f}}$) with experimental data and the results of other models for TiO_2 (15 nm) nanoparticles in ethylene glycol.

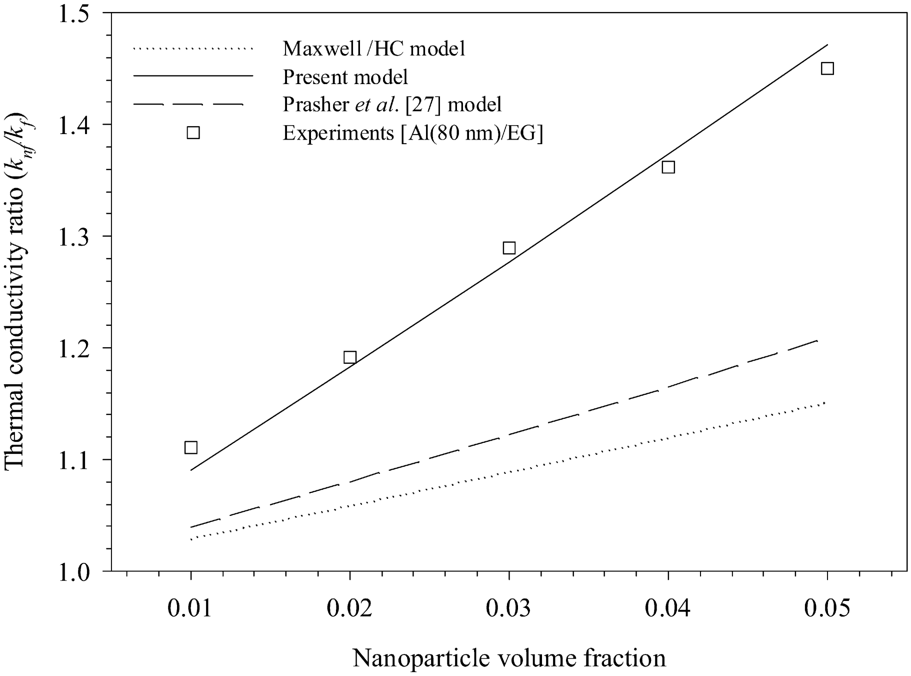

Fig. 4. Comparison of present model [Eq. (6)] predictions ($k_{\mathrm{lr}} = 3k_{\mathrm{f}}$) with experimental data and the results of other models for Al (80 nm) nanoparticles in ethylene glycol.

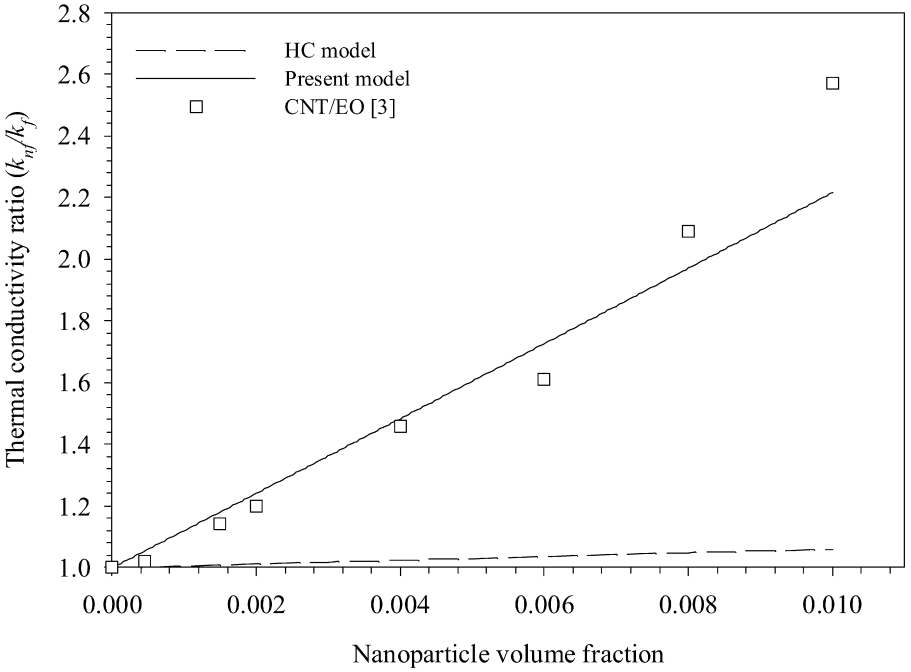

Fig. 5. Comparison of present model [Eq. (7)] predictions ($k_{\mathrm{lr}} = 60k_{\mathrm{f}}$) with experimental results of Choi et al. [3] and the results of HC model for carbon nanotubes in engine oil.

when $k_{\mathrm{p}} = 10k_{\mathrm{f}}$ or greater [13]. For CNT/EO-based nanofluids, the thermal conductivity ratio of the solid phase (CNT) to the liquid (oil) phase is very large, i.e. $k_{\mathrm{CNT}} = 13\,800k_{\mathrm{EO}}$ (where $k_{\mathrm{CNT}} = 2000\ \mathrm{W\,m^{-1}\,K^{-1}}$ and $k_{\mathrm{EO}} = 0.145\ \mathrm{W\,m^{-1}\,K^{-1}}$) [3]. In addition, as mentioned in the *Introduction*, the Hamilton–Crosser model does not take into account the effects of key factors such as the particle size and interfacial layer on the thermal conductivity of nanofluids.

From the above comparisons, it is found that adding a small volume percentage (1 to 5%) of nanoparticles in base fluids significantly increases the effective thermal conductivity of nanofluids. The proposed models show reasonably good agreement with the experimental results and give better predictions for the thermal conductivity of nanofluids compared to the existing models. This is because the present models take into account additional mechanisms such as the interfacial layer and

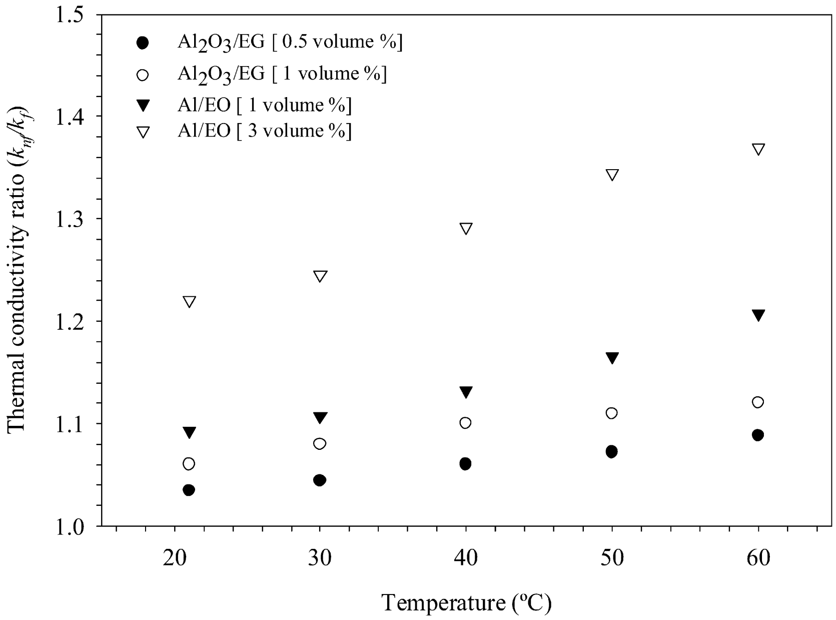

Fig. 6. Thermal conductivity enhancement with temperature for Al_2O_3 (80 nm)/ethylene glycol and Al (80 nm)/engine oil-based nanofluids.

particle size. However, the thermal conductivity of interfacial layer was chosen to be 1.25 to 3 times that of the base fluid's thermal conductivity (i.e. $k_{\mathrm{DIW}} = 0.607\ \mathrm{W\,m^{-1}\,K^{-1}}$ and $k_{\mathrm{EG}} = 0.256\ \mathrm{W\,m^{-1}\,K^{-1}}$) except for carbon nanotubes/engine oil-based nanofluids. This is because the exact thermal conductivity of the interfacial layer is not known and cannot be obtained experimentally or theoretically. However, it is presumed that the orderness and orientation of fluid molecules absorbed on the surface of particle (like surface adsorption) result in value of thermal conductivity which is intermediate between the nanoparticles and its base fluid. Moreover, the anomalous thermal conductivity of liquid film between mica plates was experimentally verified by Metsik [28]. A significant increase in the thermal conductivity of liquid film was found for water and ethyl alcohol when the thickness of liquid film reduces to 50 nm. Nevertheless, our chosen range of thermal conductivity values of interfacial layer is also consistent with the assumption made by other researchers [15,29].

The effect of temperature on the enhancement of effective thermal conductivity of nanofluids was also investigated by measuring the thermal conductivity of nanofluids for different temperatures ranging from 20–60 °C. Fig. 6 shows that at a temperature of 60 °C, the effective thermal conductivity of Al_2O_3 (80 nm)/EG based nanofluids increases by about 9% and 12% (compared to that of the base fluid) for nanoparticle volumetric loadings of 0.5% and 1%, respectively. It can also be seen that the enhancement of effective thermal conductivity of Al (80 nm)/EO nanofluids are 20% and 37% for volumetric loadings of 1% and 3% nanoparticles in the base fluid, respectively. No experimental data on the effective thermal conductivities of these nanofluids (Al_2O_3 (80 nm)/EG and Al (80 nm)/EO) with temperature are available in the literature to compare with the present experimental results. Figs. 7 and 8 compare the current experimental data for Al_2O_3/water based nanofluids at 1% volumetric loading of nanoparticles and the data reported by Das et al. [8] and Chon and Kihm [9]. It can be seen from Fig. 7 that our results are consistent with the experimental data of Das et al. and Chon and Kihm although the size of our Al_2O_3 nanoparticles is much larger than those of their nanoparticles. For the same size (150 nm) of Al_2O_3 nanoparticles, our results of thermal conductivity are slightly higher than those reported by Chon and Kihm [9] as shown in Fig. 8. The observed differences could be due to the addition of surfactant to our nanofluids and the different measurement methods. Figs. 6 to 8 demonstrate that the experimental values of thermal conductivity of different nanofluids increase significantly with the fluid temperature. This is because the high fluid temperature intensifies the Brownian motion of nanoparticles and also decreases the viscosity of the base fluid. With an intensified Brownian motion, the contribution of microconvection in heat transport increases which results in increased enhancement of the thermal conductivity of nanofluids.

The viscosity of nanofluids was also measured and found to increase with the volumetric loading of nanoparticles. Masuda et al. [19] measured the viscosity of suspensions of dispersed ultra-fine particles. For comparison, their experimental data are shown in Fig. 9. It can be seen that our measured relative viscosity data for TiO_2 (15 nm)/water based nanofluids are higher than those of Masuda et al. who showed that TiO_2 (27 nm) particles at a volume fraction of 4.3% increased the viscosity of water by 60%. Our measured viscosities of Al_2O_3 (80 nm)/DIW based nanofluids were also found to increase by nearly 82% for the maximum volumetric loading of nanoparticles 5%. A similar increment (86%) of the effective viscosity of Al_2O_3 (28 nm)/distilled water based nanofluids was also observed by Wang et al. [2] for the same volume fraction of 0.05. In their case, a mechanical blending technique was used for the dispersion of Al_2O_3 nanoparticles in distilled water. The reasons for the differences could be due to the difference in the size of the particle clusters, differences in the dispersion tech-

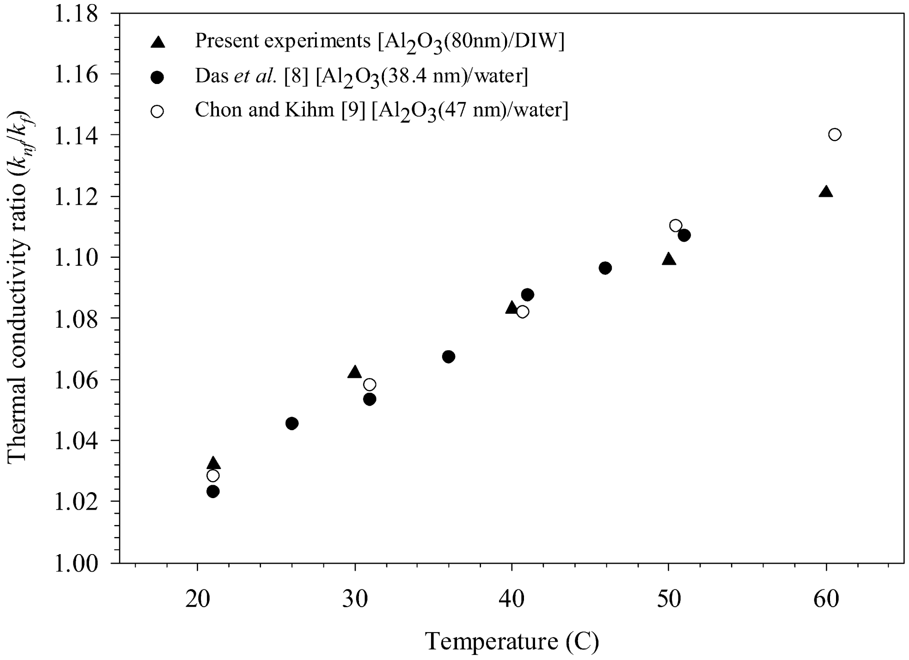

Fig. 7. Thermal conductivity enhancement with temperature for Al_2O_3/water-based nanofluids.

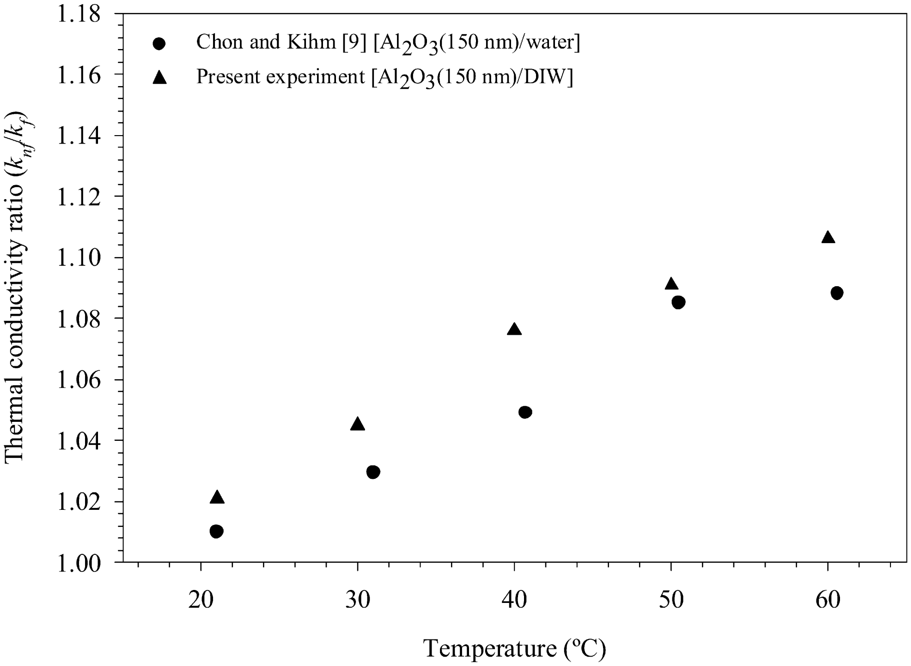

Fig. 8. Thermal conductivity enhancement with temperature for Al_2O_3 (150 nm)/water-based nanofluids.

niques and the use of surfactant in the present study. It can also be seen that the measured viscosities of nanofluids are underpredicted by two models. This is probably because these models considered only particle volume fraction, whereas the nanoparticles in fluids can easily form clusters and experience surface adsorption. Clustering and adsorption increase the hydrodynamic diameter of nanoparticles leading to the increase of relative viscosity. Besides the particle volume fraction and size, the nature of the particle surface, ionic strength of the base fluid, surfactants, pH values, inter-particle potentials such as repulsive (electric double layer force) and attractive (van der Waals force) forces may play significant role to alter the viscosity of nanofluids. However, such enhancement of viscosity may diminish the potential benefits of nanofluids. Therefore, it is imperative to conduct more comprehensive studies on the viscosity of nanofluids.

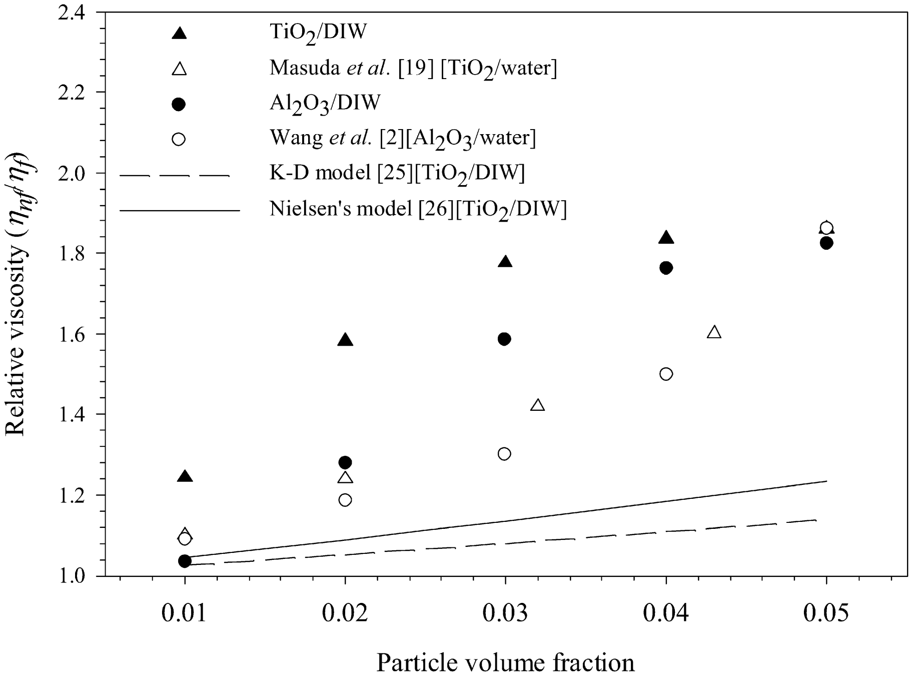

Fig. 9. Relative viscosity of nanofluids with nanoparticle volume fraction.

5. Conclusions

The effective thermal conductivity and viscosity of nanofluids were found to significantly increase with the particle volume fraction. A linear increase in the effective thermal conductivity of nanofluids with temperature was also observed. The proposed models, which consider particle size, interfacial layer, and volume fraction, show good agreement with the experimental results and give better predictions for the thermal conductivity of nanofluids compared to the existing models. Besides the volume fraction of particle, it can also be concluded that particle size, shape, interfacial layer, and temperature also influence the thermal conductivity of nanofluids. The effect of temperature on the enhanced effective thermal conductivity of nanofluids is important for theoretical understanding and needs to be considered for the model development. The enhancement of viscosity may diminish the effectiveness of nanofluids in practical applications.

References

[1] J.A. Eastman, S.U.S. Choi, S. Li, L.J. Thompson, Enhanced thermal conductivity through the development of nanofluids, in: Proceedings of the Symposium on Nanophase and Nanocomposite Materials II, vol. 457, Materials Research Society, Boston, USA, 1997, pp. 3–11.

[2] X. Wang, X. Xu, S.U.S. Choi, Thermal conductivity of nanoparticle–fluid mixture, J. Thermophys. Heat Transfer 13 (1999) 474–480.

[3] S.U.S. Choi, Z.G. Zhang, W. Yu, F.E. Lockwood, E.A. Grulke, Anomalous thermal conductivity enhancement in nanotube suspensions, Appl. Phys. Lett. 79 (2001) 2252–2254.

[4] Y. Xuan, Q. Li, W. Hu, Aggregation structure and thermal conductivity of nanofluids, AIChE J. 49 (2003) 1038–1043.

[5] C.H. Li, G.P. Peterson, Experimental investigation of temperature and volume fraction variations on the effective thermal conductivity of nanoparticle suspensions (nanofluids), J. Appl. Phys. 99 (2006) 084314.

[6] H. Zhu, C. Zhang, S. Liu, Y. Tang, Y. Yin, Effects of nanoparticles clustering and alignment on thermal conductivities of Fe_3O_4 aqueous nanofluids, Appl. Phys. Lett. 89 (2006) 023123-1–023123-3.

[7] S.M.S. Murshed, K.C. Leong, C. Yang, Enhanced thermal conductivity of TiO_2-water based nanofluids, Int. J. Thermal Sci. 44 (2005) 367–373.

[8] S.K. Das, N. Putra, P. Thiesen, W. Roetzel, Temperature dependence of thermal conductivity enhancement for nanofluids, J. Heat Transfer 125 (2003) 567–574.

[9] C.H. Chon, K.D. Kihm, Thermal conductivity enhancement of nanofluids by Brownian motion, J. Heat Transfer 127 (2005) 810.

[10] J.C. Maxwell, A Treatise on Electricity and Magnetism, third ed., Clarendon Press, Oxford, UK, 1891.

[11] R.L. Hamilton, O.K. Crosser, Thermal conductivity of heterogeneous two component systems, I & EC Fundamentals 1 (1962) 187–191.

[12] P.M. Hui, X. Zhang, A.J. Markworth, D. Stroud, Thermal conductivity of graded composites: numerical simulations and an effective medium approximation, J. Mater. Sci. 34 (1999) 5497–5503.

[13] P. Keblinski, S.R. Phillpot, S.U.S. Choi, J.A. Eastman, Mechanisms of heat flow in suspensions of nano-sized particles (nanofluids), Int. J. Heat Mass Transfer 45 (2002) 855–863.

[14] S.M.S. Murshed, K.C. Leong, C. Yang, A model for predicting the effective thermal conductivity of nanoparticle–fluid suspensions, Int. J. Nanosci. 5 (2006) 23–33.

[15] Q.-Z. Xue, Model for effective thermal conductivity of nanofluids, Phys. Lett. A 307 (2003) 313–317.

[16] W. Yu, S.U.S. Choi, The role of interfacial layers in the enhanced thermal conductivity of nanofluids: a renovated Maxwell model, J. Nanoparticle Res. 5 (2003) 167–171.

[17] W. Yu, S.U.S. Choi, The role of interfacial layers in the enhanced thermal conductivity of nanofluids: a renovated Hamilton–Crosser model, J. Nanoparticle Res. 6 (2004) 355–361.

[18] J.A. Eastman, S.R. Phillpot, S.U.S. Choi, P. Keblinski, Thermal transport in nanofluids, Annu. Rev. Mater. Res. 34 (2004) 219–246.

[19] H. Masuda, A. Ebata, K. Teramae, N. Hishinuma, Alteration of thermal conductivity and viscosity of liquid by dispersing ultra-fine particles (dispersion of Al_2O_3, SiO_2 and TiO_2 ultra-fine particles), Netsu Bussei (Japan) 4 (1993) 227–233.

[20] K.C. Leong, C. Yang, S.M.S. Murshed, A model for the thermal conductivity of nanofluids—the effect of interfacial layer, J. Nanoparticle Res. 8 (2006) 245–254.

[21] T. Hashimoto, M. Fujimura, H. Kawai, Domain-boundary structure of styrene–isoprene block copolymer films cast from solutions. 5. Molecular-weight dependence of spherical microdomains, Macromolecules 13 (1980) 1660–1669.

[22] Z.H. Li, Y.J. Gong, M. Pu, D. Wu, Y.H. Sun, J. Wang, Y. Liu, B.Z. Dong, Determination of interfacial layer thickness of a pseudo two-phase system by extension of the Debye equation, J. Phys. D: Appl. Phys. 34 (2001) 2085–2088.

[23] C.-J. Yu, A.G. Richter, A. Datta, M.K. Durbin, P. Dutta, Molecular layering in a liquid on a solid substrate: an X-ray reflectivity study, Physica B 283 (2000) 27–31.

[24] L. Xue, P. Keblinski, S.R. Phillpot, S.U.S. Choi, J.A. Eastman, Effect of liquid layering at the liquid–solid interface on thermal transport, Int. J. Heat Mass Transfer 47 (2004) 4277–4284.

[25] I.M. Krieger, T.J. Dougherty, A mechanism for non-Newtonian flow in suspensions of rigid spheres, Trans. Soc. Rheol. 3 (1959) 137–152.

[26] L.E. Nielsen, Generalized equation for the elastic moduli of composite materials, J. Appl. Phys. 41 (1970) 4626–4627.

[27] R.S. Prasher, P. Bhattacharya, P.E. Phelan, Thermal conductivity of nanoscale colloidal solutions (nanofluids), Phys. Rev. Lett. 94 (2005) 025901-1–025901-4.

[28] M.S. Metsik, Properties of water films between mica plates, in: B.V. Deryagin (Ed.), Research in Surface Forces, in: Surface Forces in Thin Films and Disperse Systems, vol. 4, Consultants Bureau, New York, 1975.

[29] H. Xie, M. Fujii, X. Zhang, Effect of interfacial nanolayer on the effective thermal conductivity of nanoparticle–fluid mixture, Int. J. Heat Mass Transfer 48 (2005) 2926–2932.